

Unroofing the core of the central Andean fold-thrust belt during focused late Miocene exhumation: evidence from the Tipuani-Mapiri wedge-top basin, Bolivia

Jesse G. Mosolf,* Brian K. Horton,† Matthew T. Heizler‡ and Ramiro Matos§

*Department of Earth Science, University of California, Santa Barbara, CA, USA

†Institute for Geophysics and Department of Geological Sciences, Jackson School of Geosciences, University of Texas at Austin, Austin, TX, USA

‡New Mexico Bureau of Geology and Mineral Resources, Socorro, NM, USA

§Instituto de Investigaciones Geológicas y Medio Ambiente, Universidad Mayor de San Andrés, La Paz, Bolivia

ABSTRACT

As the highest part of the central Andean fold-thrust belt, the Eastern Cordillera defines an orographic barrier dividing the Altiplano hinterland from the South American foreland. Although the Eastern Cordillera influences the climatic and geomorphic evolution of the central Andes, the interplay among tectonics, climate and erosion remains unclear. We investigate these relationships through analyses of the depositional systems, sediment provenance and $^{40}\text{Ar}/^{39}\text{Ar}$ geochronology of the upper Miocene Cangalli Formation exposed in the Tipuani-Mapiri basin (15–16°S) along the boundary of the Eastern Cordillera and Interandean Zone in Bolivia. Results indicate that coarse-grained nonmarine sediments accumulated in a wedge-top basin upon a palaeotopographic surface deeply incised into deformed Palaeozoic rocks. Seven lithofacies and three lithofacies associations reflect deposition by high-energy braided river systems, with stratigraphic relationships revealing significant (~500 m) palaeorelief. Palaeocurrents and compositional provenance data link sediment accumulation to pronounced late Miocene erosion of the deepest levels of the Eastern Cordillera. $^{40}\text{Ar}/^{39}\text{Ar}$ ages of interbedded tuffs suggest that sedimentation along the Eastern Cordillera–Interandean Zone boundary was ongoing by 9.2 Ma and continued until at least ~7.4 Ma. Limited deformation of subhorizontal basin fill, in comparison with folded and faulted rocks of the unconformably underlying Palaeozoic section, implies that the thrust front had advanced into the Subandean Zone by the 11–9 Ma onset of basin filling. Documented rapid exhumation of the Eastern Cordillera from ~11 Ma onward was decoupled from upper-crustal shortening and coeval with sedimentation in the Tipuani-Mapiri basin, suggesting climate change (enhanced precipitation) or lower crustal and mantle processes (stacking of basement thrust sheets or removal of mantle lithosphere) as possible controls on late Cenozoic erosion and wedge-top accumulation. Regardless of the precise trigger, we propose that an abruptly increased supply of wedge-top sediment produced an additional sedimentary load that helped promote late Miocene advance of the central Andean thrust front in the Subandean Zone.

INTRODUCTION

The Eastern Cordillera in the central Andes achieves mean elevations over ~5 km and creates an orographic barrier between the internally drained Altiplano hinterland basin and externally drained foreland river systems (Fig. 1). In Bolivia, the Eastern Cordillera exposes the deepest levels of the central Andean fold-thrust belt and defines the transition from hinterland- to foreland-directed thrust

structures (Gillis *et al.*, 2006; McQuarrie *et al.*, 2008a). Topography of the Eastern Cordillera steps down rapidly towards the < 1 km elevations of the Interandean Zone and Subandean Zone (Fig. 1); this high relief profoundly influences orographic precipitation, regional climate and geomorphic evolution of the central Andes (Masek *et al.*, 1994; Horton, 1999; Montgomery *et al.*, 2001; Barnes & Pelletier, 2006). However, the interplay of tectonics, climate and erosion (e.g. Uba *et al.*, 2007; McQuarrie *et al.*, 2008b) remains unresolved in this humid, high-relief region. Interestingly, mapping and thermochronology show that the ~11 Ma onset of youthful exhumation in the Eastern

Correspondence: Jesse G. Mosolf, Department of Earth Science, University of California, Santa Barbara, CA 93106-9630, USA. E-mail: jmosolf@umail.ucsb.edu

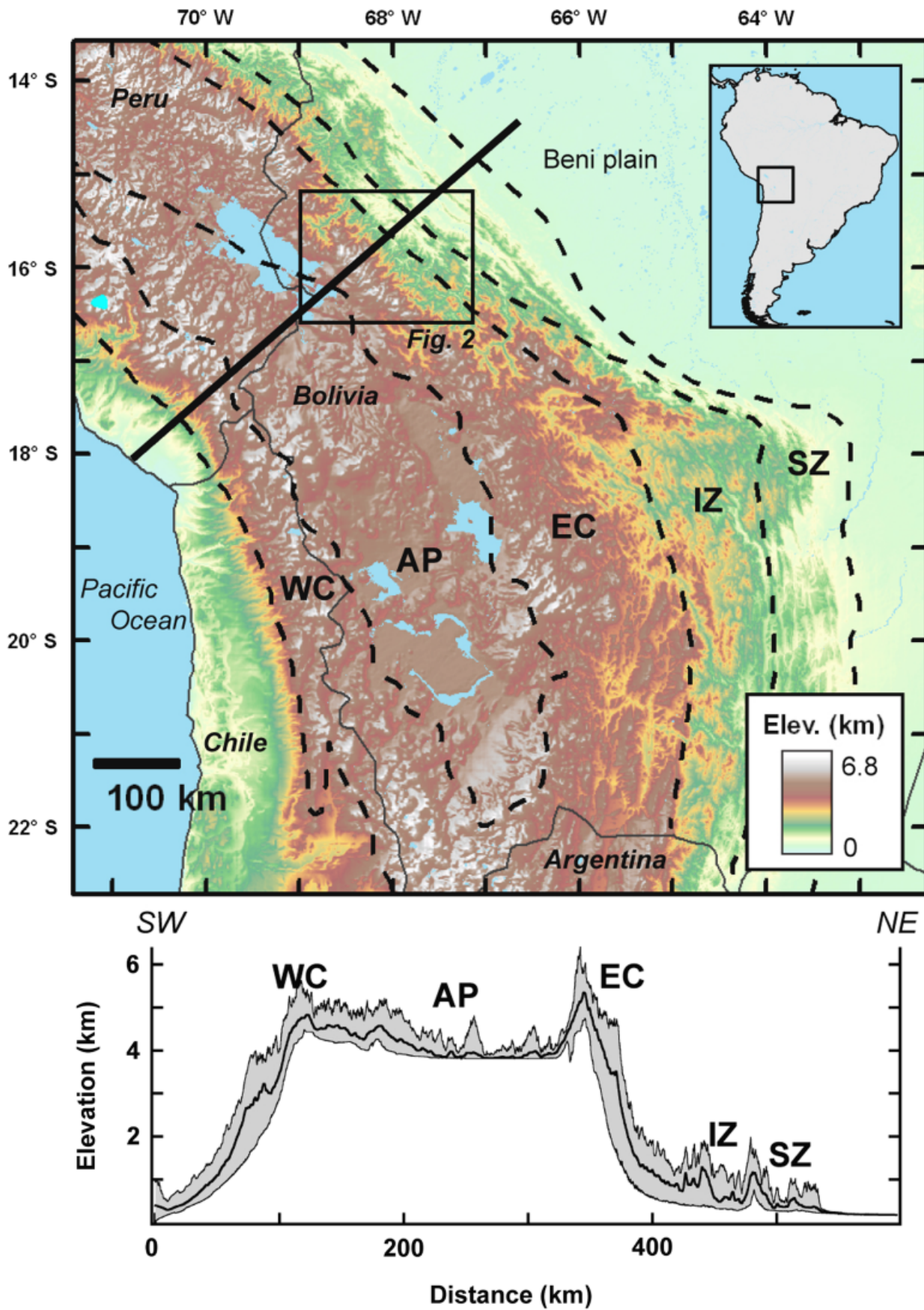


Fig. 1. Map and cross section showing regional topography of the central Andes, including the Western Cordillera (WC), Altiplano (AP), Eastern Cordillera (EC), Interandean Zone (IZ) and Subandean Zone (SZ). Topographic cross section was extracted from SRTM DEM (40 km wide swath). Modified from Isacks (1988), Masek *et al.* (1994) and McQuarrie *et al.* (2005).

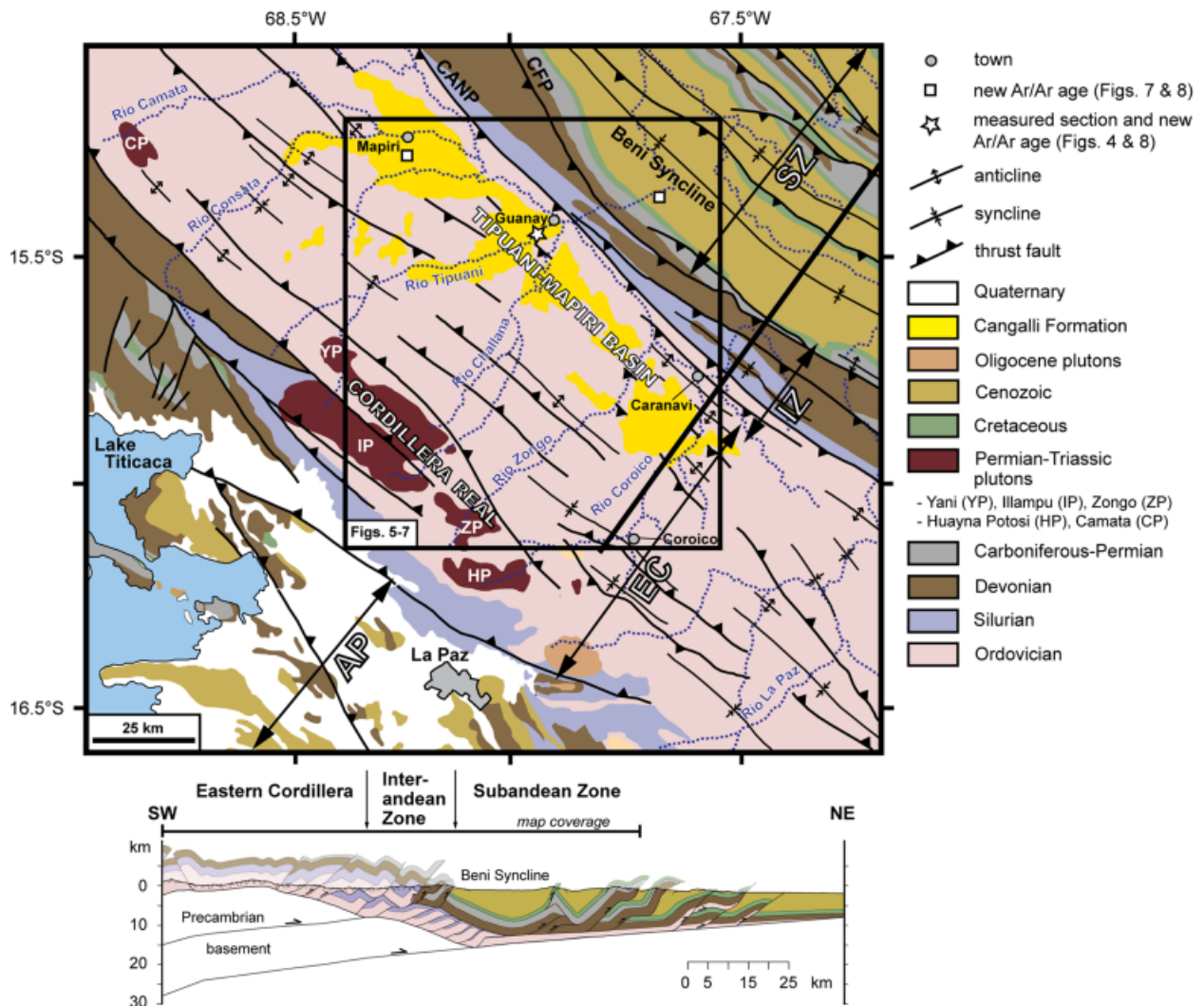


Fig. 2. Geologic map and cross section showing geologic units, structures, and modern rivers of the Tipuani-Mapiri basin and surrounding regions, including the easternmost Altiplano (AP), Eastern Cordillera (EC), Interandean Zone (IZ) and Subandean Zone (SZ). Map simplified from Servicio Nacional de Geología y Minería (1990), Fornari *et al.* (1987), and McQuarrie *et al.* (2008a) depicts general structures, including the principal Interandean structures (CANP, Main Andean thrust; CFP, Main Frontal thrust). Balanced cross section from McQuarrie *et al.* (2008a) depicts a greater level of detail and an interpretation of two basement thrust sheets.

Cordillera occurred after local upper-crustal shortening ceased in early Miocene time (Gillis *et al.*, 2006). Such decoupling of late Cenozoic exhumation from upper-crustal shortening allows for better evaluation of the effects of climate variability and deeper crustal/lithospheric dynamics on erosion and topography.

Here we investigate exhumation of the Eastern Cordillera through stratigraphic and sedimentologic observations, sediment provenance and $^{40}\text{Ar}/^{39}\text{Ar}$ geochronology of Neogene strata (Cangalli Formation) in the Tipuani-Mapiri basin (Fig. 2) (Fornari *et al.*, 1987; Herail *et al.*, 1989). This study reports: (1) stratigraphic and sedimentologic descriptions characterizing the palaeotopography and depositional conditions for the Tipuani-Mapiri basin; (2) sediment provenance data (conglomerate clast counts and palaeocurrent results) linking basin fill to exhumation of the Eastern Cordillera; and (3) $^{40}\text{Ar}/^{39}\text{Ar}$ ages for tuffs constraining the punctuated accumulation history of the basin. Integration

of stratigraphic, structural and $^{40}\text{Ar}/^{39}\text{Ar}$ results helps elucidate the timing of deposition and upper-crustal shortening, yielding insights into the tectonic and topographic evolution of the central Andean fold-thrust belt.

GEOLOGIC BACKGROUND

Regional setting

Cenozoic east-west shortening in Bolivia generated an eastward advancing fold-thrust belt linked to crustal thickening and rise of the central Andean plateau (Isacks, 1988; Sempere *et al.*, 1990; Gubbels *et al.*, 1993; Allmendinger *et al.*, 1997; Baby *et al.*, 1997; McQuarrie, 2002; Barke & Lamb, 2006). The central Andes are divided into the Western Cordillera, Altiplano, Eastern Cordillera, Interandean Zone and Subandean Zone (Fig. 1). The Western Cordillera

magmatic arc defines the Altiplano–Pacific drainage divide and contains volcanic peaks reaching 5–6.5 km. To the east, the Altiplano is an internally drained basin with average elevation of 3.8 km. The Eastern Cordillera (4–5 km average elevation) is a bivergent thrust system composed of shortened Palaeozoic strata and granitic plutons. In the Eastern Cordillera, the boundary between a hinterland-directed backthrust belt and foreland-directed structures to the east is approximated by the single highest (4–6.4 km) range, the Cordillera Real, at 15.5–17.5°S (Fig. 2) (Roeder, 1988; Gillis *et al.*, 2006; McQuarrie *et al.*, 2008a). Towards the foreland, elevation decreases rapidly into the Interandean Zone, a region of deformed Palaeozoic strata, and the adjacent Subandean Zone, the frontal, craton-directed region of the central Andean fold-thrust belt.

The Neogene Cangalli Formation was deposited in the Tipuani–Mapiri basin at 15–16°S, a 30 × 120 km belt of NNW-trending outcrops along the boundary zone between the Eastern Cordillera and Interandean Zone (Figs 1 and 2). Relationships are poorly constrained between basin evolution and Interandean fault systems near the basin’s NE margin, including structures occasionally referred to as the Main Andean thrust (or Cabalgamiento Andino Principal; CANP) and Main Frontal thrust (or Cabalgamiento Frontal Principal; CFP). Up to 1 km of nonmarine basin fill unconformably overlies deformed Ordovician rocks, fossilizing a complex palaeotopography

(Fornari *et al.*, 1987). The coarse-grained clastic fill reportedly sustained limited deformation (Heraill *et al.*, 1989), implying deposition after the principal phase of shortening along the Eastern Cordillera–Interandean Zone boundary.

Shortening and exhumation

Crustal shortening estimates in Bolivia range from 200 to 350 km (Sheffels, 1990; Schmitz, 1994; Baby *et al.*, 1997; Kley & Monaldi, 1998; McQuarrie & DeCelles, 2001; McQuarrie, 2002; McQuarrie *et al.*, 2008a). The kinematic history of this shortening remains contested. One viewpoint invokes distributed deformation across the Eastern Cordillera commencing at ~27 Ma, followed by intense deformation in the Subandean Zone after ~10 Ma, coeval with plateau uplift (Isacks, 1988; Sempere *et al.*, 1990; Gubbels *et al.*, 1993; Allmendinger *et al.*, 1997). An alternative view involves gradual uplift achieved by protracted shortening during eastward advance of deformation since early Cenozoic time (Lamb & Hoke, 1997; DeCelles & Horton, 2003; McQuarrie *et al.*, 2005; Barnes *et al.*, 2008).

Inferences from structural relationships, basin fill, and thermochronology suggest that shortening was underway during the Eocene (Benjamin *et al.*, 1987; Farrar *et al.*, 1988; Elger *et al.*, 2005; Horton, 2005; Barnes *et al.*, 2006, 2008; Gillis *et al.*, 2006; Ege *et al.*, 2007; McQuarrie *et al.*, 2008a).

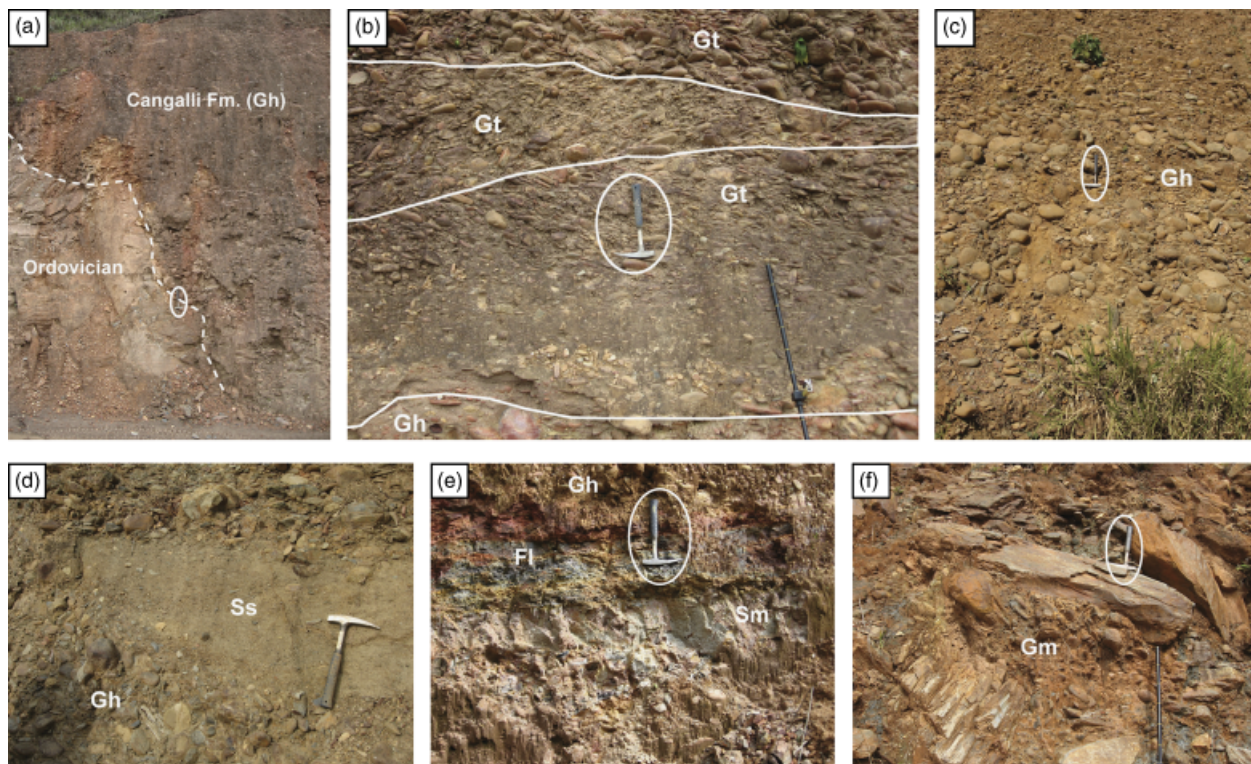


Fig. 3. Photographs of representative lithofacies, with hammer for scale. (a) Unconformable contact between deformed Ordovician strata and channelized, horizontally stratified conglomerate (Gh). (b) Trough cross-stratified pebble-cobble conglomerate (Gt) of facies association 1 displaying erosive bases of stacked channel packages. (c) Organized, weakly imbricated cobble conglomerate (Gh) of facies associations 1. (d) Interbedded pebble-cobble conglomerate (Gh) and scour-fill sandstone (Ss) of facies association 1. (e) Interbedded massive sandstone (Sm) and claystone (Fl) of facies association 2. (f) Disorganized boulder conglomerate of facies association 3.

Cenozoic deposits in the Altiplano and Eastern Cordillera provide evidence for foreland basin development, thus suggesting shortening-induced crustal loading and flexure, by middle Eocene time (Horton *et al.*, 2001, 2002; DeCelles & Horton, 2003). Rapid exhumation presumably related to upper-crustal shortening in the central Andean backthrust belt occurred from middle Eocene to early Miocene time (Gillis *et al.*, 2006; Leier *et al.*, 2010; Murray *et al.*, 2010), implying the thrust front had propagated farther eastward by 25–20 Ma. However, cross-cutting relationships suggest that a younger, late Miocene phase of rapid exhumation postdates local shortening and eastward advance of the thrust front (Gillis *et al.*, 2006). Fission track and (U–Th)/He ages record exhumation in the Interandean Zone as early as 30–25 Ma, followed by distributed exhumation across the fold-thrust belt after ~15 Ma (Barnes *et al.*, 2006; Ege *et al.*, 2007; McQuarrie *et al.*, 2008a). These relationships suggest that the Tipuani–Mapiri basin may shed

light on both pre- and postshortening histories of exhumation in the transition zone encompassing the Eastern Cordillera, Interandean Zone and Subandean Zone.

DEPOSITIONAL SYSTEMS

Stratigraphic context

The Tipuani–Mapiri basin (Fig. 2) is primarily composed of subhorizontal conglomerates deposited in drainages incised into underlying Palaeozoic strata (Fornari *et al.*, 1987). The Cangalli Formation rests in angular unconformity upon Ordovician strata, with onlap relationships (Fig. 3a) and an altitudinal range for the basal contact revealing an incised palaeotopography with local relief > 500 m. Previous reports suggest the Cangalli Formation may have attained a thickness of 1 km (Herail *et al.*, 1994), but much of the succession has since been dissected and eroded within

Table 1. Description and interpretation of sedimentary lithofacies (after Miall, 1985; Uba *et al.*, 2005)

| Facies code | Description | Interpretation |
|-------------|--|---|
| Gh | Organized, clast-supported, polymict conglomerate, pebbles and cobbles, rounded clasts, poor to moderate sorting, crude horizontal stratification, moderate imbrication, weak normal grading | Longitudinal bar, traction bedload |
| Gt | Clast-supported, trough-cross stratified, polymict conglomerate, pebbles and cobbles, subrounded to rounded clasts, poor to moderate sorting, normal grading | Transverse bar, channel fill |
| Gm | Disorganized, clast-supported, polymict conglomerate. Pebbles to boulders, angular to subrounded clasts, no imbrication, rare normal grading | Clast-rich debris flow |
| Ss | Massive, moderately to well-sorted, very fine- to very coarse-grained sandstone, basal bedding contacts define concave-up erosive surfaces | Channel scour fill |
| Sh | Horizontally stratified sandstone, fine- to very coarse-grained, occasionally pebbly, common normal grading | Sheetflow, upper flow regime plane-bed conditions |
| Sm | Very fine- to coarse-grained sandstone, massive, tabular beds, irregular mottling and variegated colour banding | Sheetflow, hyperconcentrated flow, limited pedogenesis |
| Fl | Siltstone and claystone, thinly laminated or massive, tabular, variegated colour banding, minor mottling and soil aggregates (peds) | Suspension fallout from waning flows, limited pedogenesis |

Table 2. Description and interpretation of lithofacies associations

| Facies association | Lithofacies | Characteristics | Interpretation |
|--------------------|-------------|--|---|
| 1 | Gh, Gt, Ss | Multistorey packages of organized, stratified, commonly imbricated conglomerates with isolated, thin- to medium-bedded scour-fill sandstones | Gravel bars and channel-fill sands deposited in braided rivers |
| 2 | Sh, Sm, Fl | Interbedded, laterally extensive units of sandstone, siltstone and claystone with massive to finely laminated texture | Waning overbank sheetflow and suspension fallout in floodplains and localized lakes of braided river systems |
| 3 | Gm, Gh | Disorganized, clast-rich conglomerates displaying no internal stratification, with minor occurrences of crudely stratified, weakly imbricated conglomerate | Debris flows initiated on steep local slopes or alluvial fans, with rapid deposition in braided river systems and minor reworking |

modern watersheds. Remnants of what was once a laterally extensive conglomeratic succession occur as outcrops that flank the slopes of modern river drainages or cap palaeoridges cut into the Ordovician section. Lateral facies variations within the Cangalli Formation, as well as the complex palaeotopography preserved along the basal contact, preclude simple correlation of exposed stratigraphic successions across the Tipuani-Mapiri basin. Nevertheless, the consistently low stratal dips (generally 10°) allow for relative discrimination of lower and upper levels of the formation. Locally, basin fill is cut by high-angle faults with small amounts of reverse offset (1 m) and minor associated tilting. The relatively nondeformed character of the Cangalli Formation represents a sharp contrast from the high degree of folding, faulting and low-grade metamorphism recorded in the underlying Ordovician section (e.g. Martinez, 1980; McQuarrie & Davis, 2002). Moreover, in all localities observed throughout the boundary zone between the Eastern Cordillera and Interandean Zone, the regional-scale thrust faults within the Ordovician section do not cut the conglomeratic fill of the Tipuani-Mapiri basin (Fig. 2).

Lithofacies associations

Detailed sedimentological observations were carried out mostly along road outcrops, river cuts and placer gold-mining operations between the Consata and Coroico rivers (Fig. 2). Seven lithofacies and three lithofacies associations (Tables 1 and 2) were identified for the Cangalli Formation. Individual facies codes are modified from standard terminology for clastic nonmarine deposits (Miall, 1977, 1985, 1996; Uba et al., 2005). Lithofacies photographs (Fig. 3) and a measured section (Fig. 4) illustrate the sedimentological features and stratigraphic organization.

Lithofacies association 1. Pebble-cobble conglomerate and interbedded sandstone

Description. Dominating the basin, facies association 1 is comprised of organized polymict conglomerate (lithofacies Gh, Gt) interbedded with moderately to well-sorted sandstone (lithofacies Ss). Internally stratified, normally graded beds of conglomerate consist of imbricated clasts of subrounded to rounded pebbles and cobbles (Fig. 3b and c). Clast-supported conglomerate beds with erosive basal contacts are up to 1 m thick, extend laterally for 10–20 m and have crude horizontal stratification (lithofacies Gh). Some beds are trough-cross-stratified (lithofacies Gt) with thicknesses reaching 1 m and stacked multistorey channel-fill conglomerates forming packages ~10 m thick. Intercalated massive sandstones (lithofacies Ss) consist of very fine- to very coarse-grained sand that is moderately to well-sorted and preserved in channels ~1 m thick with a lateral extent of 1–2 m (Fig. 3d).

Interpretation. Facies association 1 is attributed to gravel deposition in a braided river system with minor accumula-

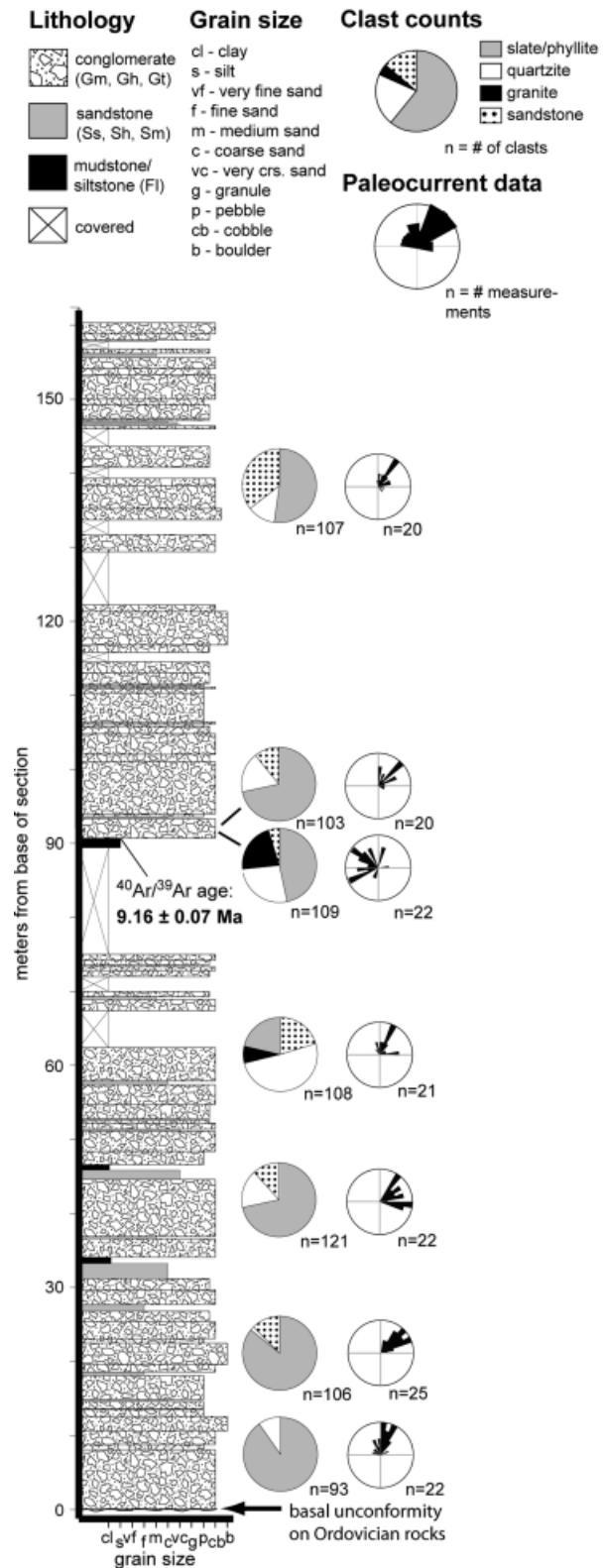


Fig. 4. Measured stratigraphic section illustrating sedimentological features and stratigraphic organization, including facies types, palaeocurrents, conglomerate clast compositions and $^{40}\text{Ar}/^{39}\text{Ar}$ ages.

tion of channel-fill sand (Miall, 1977, 1996; Jones et al., 2001; Limarino et al., 2001; Nichols & Fisher, 2007). Conglomerate beds were deposited during high-velocity

stream flows with low sediment concentrations (Miall, 1996). Stream velocities likely fluctuated, with periodic or seasonal maximum flows moving sediment by traction transport. Waning-flow/flood conditions or stream expansion resulted in reduction of stream power and formation of gravel bars, with low-relief longitudinal bars most common (Miall, 1996). Trough-cross-stratified conglomerate was formed by transverse-migrating bars in stream channels during periods of relatively high flow. Channel-fill sandstone (lithofacies *Ss*) was deposited during waning stream flow (Uba *et al.*, 2005), filling channel scours cut into gravel bars during high-velocity stream flow. The relative abundance of facies association 1 suggests the bulk of the Cangalli Formation was deposited in high-energy, low-sinuosity, braided stream environments, possibly in the proximal sectors of fluvial megafans (e.g. Horton & DeCelles, 2001; Uba *et al.*, 2005).

Lithofacies association 2. Sandstone and mudstone

Description. Facies association 2 (Fig. 3e) is composed of sandstone, siltstone and claystone. The sandstone consists of massive, moderately to well-sorted, fine- to very coarse-grained sand (lithofacies *Sm*). Tabular beds are up to 2 m thick, extend laterally for tens of metres and have sheet geometries. Other sandstones are horizontally stratified (lithofacies *Sh*), with bed thicknesses reaching 0.5 m and extending short distances (up to ~5 m) laterally. *Sh* beds are often normally graded with pebble stringers up to 5 cm thick. Sandstone beds are commonly capped by siltstone and claystone (lithofacies *Fl*). *Fl* beds are massive or thinly laminated, up to 1 m thick and have tabular, sheet geometries over tens of metres. *Fl* beds are commonly scoured by overlying conglomerate beds, forming irregular and undulatory bedding contacts. Many mudstones, and some sandstones of this facies association, are mottled with variegated colour bands.

Interpretation. Facies association 2 is interpreted as overbank and localized lacustrine sediments deposited on floodplains of a braided river system, possibly during overtopping of channel margins during flood events (Jones *et al.*, 2001; Limarino *et al.*, 2001; Mack *et al.*, 2003; Uba *et al.*, 2005). Breaching of channel margins resulted in waning-flow and crevasse-splay deposition of massive to horizontally stratified sand (lithofacies *Sh* and *Sm*). *Fl* beds were deposited from suspension on the fluvial floodplains during waning flow conditions (Miall, 1996; Jones *et al.*, 2001; Limarino *et al.*, 2001). Small lakes and ponds may also have promoted deposition of finely laminated mud through suspension fall-out. Mottling, variegated colours and preservation of consolidated soil material (peds) suggest minor pedogenesis between events of flooding and stream migration or avulsion.

Lithofacies association 3. Cobble-boulder conglomerate

Description. Facies association 3 is the least common facies association (<10% volumetrically) and is composed of

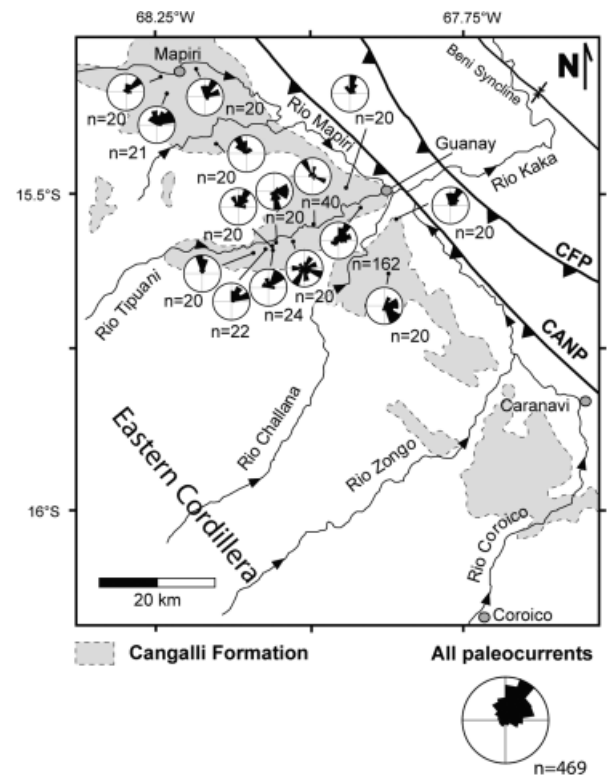


Fig. 5. Regional map showing palaeocurrent data from imbricated conglomerates of the Tipuani-Mapiri basin.

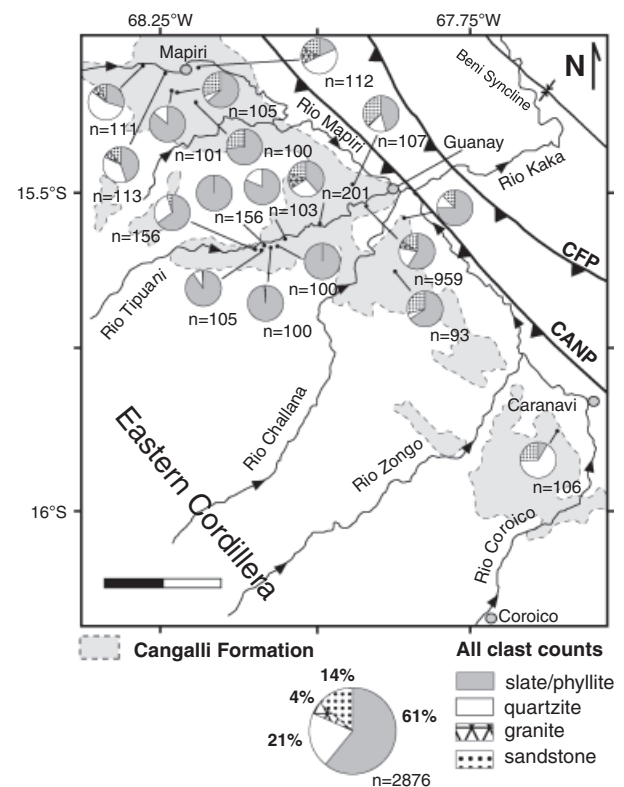


Fig. 6. Regional map showing conglomerate clast-count data for the Tipuani-Mapiri basin.

poorly sorted, angular to subrounded, clast-supported, cobble-boulder conglomerate and local breccia (lithofacies *Gm*). Polymict clasts are up to ~ 1 m in diameter and not imbricated (Fig. 3f). Individual beds are massive, up to ~ 5 m thick, and have sheet geometries that extend for tens of metres. Basal contacts are typically defined by planar nonerosive surfaces but occasionally have broad irregular surfaces. In some cases, disorganized conglomerate beds, which lack internal stratification, grade upward into better organized conglomerates exhibiting crude horizontal stratification, imbrication and normal grading (lithofacies *Gh*). Deposits of facies association 3 are generally interbedded with, or can be traced laterally into, facies association 1.

Interpretation. Facies association 3 is interpreted to represent clast-rich debris flows initiated on local steep channel flanks or on small alluvial fans flanking braided stream systems (Blair & McPherson, 1992, 1994; Miall, 1996). Close association of debris-flow conglomerates with better organized deposits of facies association 1 suggests mobilization within a braided river system exhibiting locally high relief or small, short-lived alluvial fans. Minimal channelization and a lack of organized sedimentary structures suggest that these poorly sorted conglomerates were rapidly deposited in sheet geometries from high viscosity, sediment-concentrated flows (Blair & McPherson, 1994). The debris flows were likely generated by mobilization of colluvium into braided channels and their associated floodplains. In some cases, minor flow modification within channels resulted in limited horizontal stratification, clast imbrication and normal grading.

PROVENANCE

Sediment dispersal patterns

Palaeocurrent assessments of Tipuani-Mapiri basin fill enable a comparison with modern drainage patterns to determine if structural barriers along the Interandean Zone-Subandean Zone boundary guided sedimentation pathways. The present drainage system shows considerable structural influence. Specifically, the Eastern Cordillera (Fig. 2) exhibits a modern trellis drainage system consisting of transverse, NE-flowing tributary rivers (e.g. Rios Camata, Consata, Tipuani, Challana, Zongo, Coroico and La Paz) that join major axial, NW- and SE-flowing rivers parallel to regional tectonic strike. The consistent position of axial rivers (such as the SE-flowing Rio Mapiri and NW-flowing lower Rio Coroico) parallel to the Main Andean thrust (CANP) and Main Frontal thrust (CFP) reveals a structural control on modern drainage (Fig. 2).

Palaeocurrent data for the Cangalli Formation (Fig. 5) were collected from imbricated clasts in cobble conglomerates (lithofacies *Gh*, *Gt*). A total of 469 measurements were made at 15 localities, including a single locality with 162 measurements. Collectively, the data reveal a prevailing palaeoflow direction from SW to NE. The calculated mean

palaeocurrent azimuth remains remarkably consistent whether all 469 measurements are weighted equally (029°), all 15 localities are weighted equally (032°), or the locality with 162 measurements is excluded (031°). There is moderate variability in palaeoflow among localities (Fig. 5), but few well-defined spatial or temporal trends. The data do not exhibit systematic changes over the ~ 60 km distance along strike, or from lower to upper stratigraphic levels. The palaeocurrent data also show some limited evidence of axial palaeoflow comparable to the modern, structurally controlled SE- and NW-flowing rivers adjacent to the CANP fault system (Fig. 2). Overall; however, sediment dispersal during basin filling was principally from SW to NE, transverse to regional tectonic strike.

Conglomerate clast compositions

Compositional data are derived from counts of 2876 individual clasts at 18 localities (Fig. 6). Clast-count data were grouped into four general categories, including slate/phyllite, quartzite, sandstone and granite. The dominant slate/phyllite category accounts for 61% of counted clasts (Fig. 6). Quartzite, sandstone and granite categories account for 21%, 14% and 4% of the data, respectively. The source of slate/phyllite, quartzite and sandstone clasts can be linked to the Ordovician Coroico and Amutara, the Devonian Vila Vila and the Silurian Uncia and Catavi formations (GEOBOL, 1994, 1995). Granite clasts are diagnostic of plutons in the Eastern Cordillera to the west. Because other granites are hundreds of kilometres away in the Western Cordillera or eastern craton, granite clasts are considered to unequivocally link the Cangalli Formation to

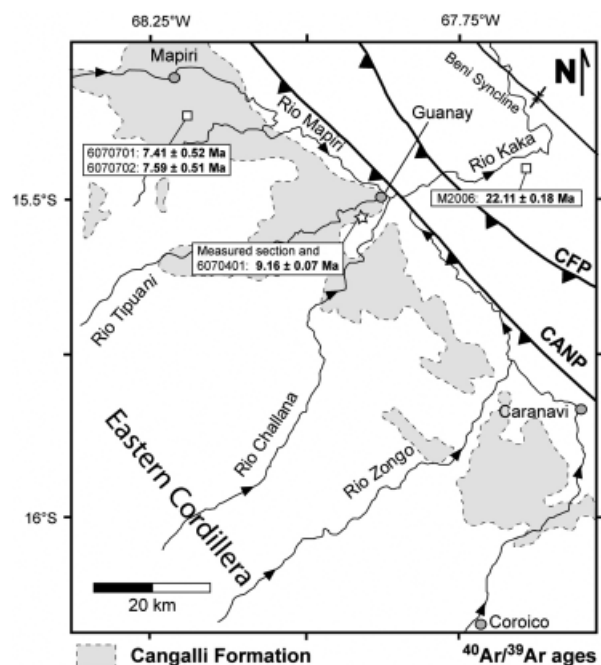


Fig. 7. Regional map showing location of $^{40}\text{Ar}/^{39}\text{Ar}$ tuff samples (6070401, 6070701, 6070702 and M2006) and measured section (Fig. 4) in the Tipuani-Mapiri basin.

erosion of deeper levels of the western Eastern Cordillera (Cordillera Real), where Permo-Triassic and Cenozoic granites are exposed (Fig. 2) (McBride *et al.*, 1983; Gillis *et al.*, 2006). On the basis of palaeocurrent orientations (Fig. 5), granite clasts in southern outcrops along the Rio Tipuani were most likely derived from the Permo-Triassic Illampu and Yani plutons, with granite clasts in Rio Mapiri outcrops originating from isolated northern granites such as the Camata pluton (Fig. 2).

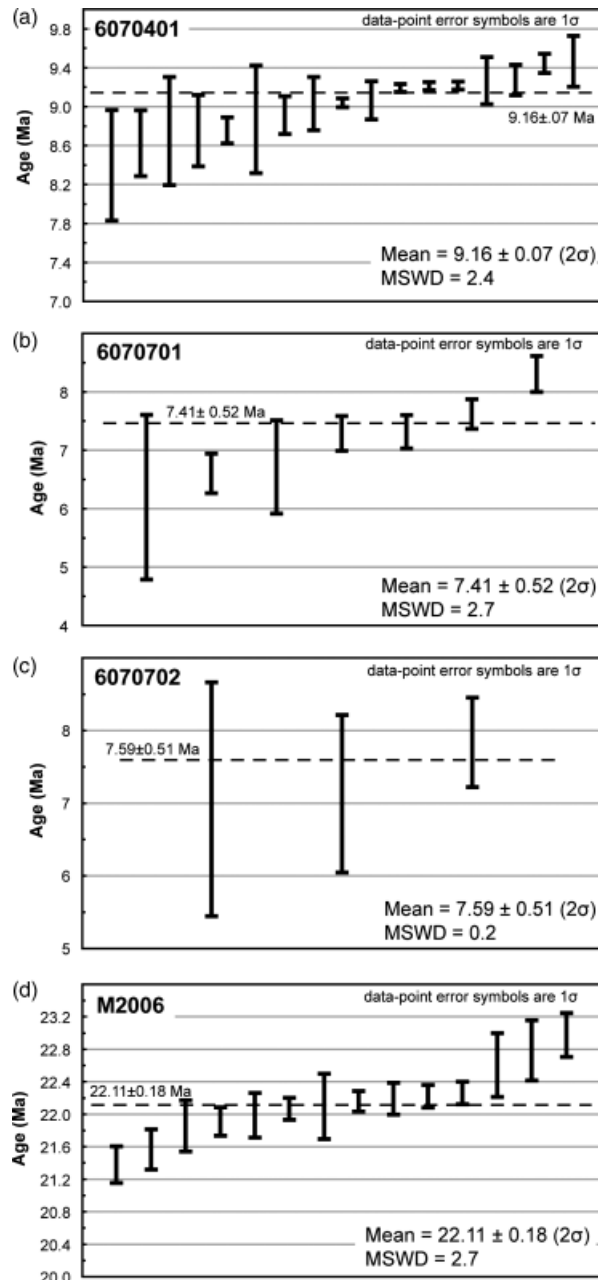


Fig. 8. Plots depicting laser total-fusion $^{40}\text{Ar}/^{39}\text{Ar}$ ages for individual sanidine crystals from four tuff samples: (a) 6070401, (b) 6070701 and (c) 6070702 from the Cangalli Formation (Eastern Cordillera–Interandean Zone) and (d) M2006 from the Mayaya region (Subandean Zone). In each plot, vertical lines represent 1 σ error bars for individual crystal ages and the dashed horizontal line represents the calculated weighted mean age (2 σ) for each sample. See Table S1 for individual $^{40}\text{Ar}/^{39}\text{Ar}$ analyses.

Although no significant stratigraphic trends in clast compositions are ascertained (Fig. 4), a spatial variability can be linked to potential source lithologies. Conglomerates observed in the northernmost (Rio Camata) and southernmost (Rio Coroico) zones of the Tipuani–Mapiri basin show greater proportions of quartzite and sandstone clasts. This pattern is potentially the product of an exposure pattern in which structurally higher levels, notably Devonian quartzites and sandstones, are preferentially preserved along strike in the northern and southern parts of the Eastern Cordillera (Fig. 2).

$^{40}\text{Ar}/^{39}\text{Ar}$ GEOCHRONOLOGY

$^{40}\text{Ar}/^{39}\text{Ar}$ results

Ash-fall tuffs were collected at two localities in the Tipuani–Mapiri basin (Fig. 7). The southern locality (sample 6070401), along the Rio Tipuani near the Merma mine SW of Guanay, represents lower stratigraphic levels of the basin. The northern locality (sample 607071), along the Rio Consata in the Chontalaruni drainage near Vilaque, represents the upper levels of the Cangalli Formation.

$^{40}\text{Ar}/^{39}\text{Ar}$ laser total-fusion analyses were performed at the New Mexico Geochronology Research Laboratory on sanidine crystals separated from each sample. $^{40}\text{Ar}/^{39}\text{Ar}$ results for individual sanidine crystals were used to calculate a weighted mean age for each sample (Fig. 8). Sample 6070401 yields a weighted mean age of 9.16 ± 0.07 Ma (2 σ) on the basis of 17 individual grain ages. For sample 6070701, individual ages of seven sanidine grains yield a weighted mean age of 7.41 ± 0.52 Ma (2 σ). $^{40}\text{Ar}/^{39}\text{Ar}$ analyses of three sanidine grains from sample 6070702, from the same stratigraphic level, yield a similar but less precise weighted mean age of 7.59 ± 0.51 Ma (2 σ). The ages reported here are in agreement with previous studies. Although no analytical results were published, Fornari *et al.* (1987) and Herail *et al.* (1989, 1994) reported a K–Ar age of ~ 9 Ma (no error bars listed) and $^{40}\text{Ar}/^{39}\text{Ar}$ ages of 7.79 ± 0.03 and 7.96 ± 0.06 Ma.

$^{40}\text{Ar}/^{39}\text{Ar}$ analyses were also conducted for a single tuff, sample M2006, from the lower levels of the clastic succession in the Beni syncline of the Subandean Zone, ENE of Guanay (Figs 2 and 7). Although the Charqui Formation of the Subandean Zone could be regarded as possible distal equivalents of Tipuani–Mapiri basin fill, analyses of 14 sanidine grains yield a weighted mean age of 22.11 ± 0.18 Ma, substantially older than the Cangalli Formation but consistent with the reported age of the Quendeque Formation in the Subandean Zone (Strub *et al.*, 2005).

Interpretations

$^{40}\text{Ar}/^{39}\text{Ar}$ ages for tuffs provide a minimum depositional age for the Cangalli Formation. Sample 6070401 (9.16 ± 0.07 Ma) was taken from the lower part of the formation, ~ 90 m above the basal contact (Fig. 4). This

sample provides a minimum age of 9.2 Ma for initial sedimentation in the Tipuani–Mapiri basin and the cessation of upper-crustal shortening along the Eastern Cordillera–Interandean Zone boundary. The absence of recognizable growth strata and shortening-related deformation in the Cangalli Formation further implies that the thrust front had advanced towards the foreland, NE of the Tipuani–Mapiri basin, by the time of initial basin infilling at 9.2 Ma. Although there are no direct age constraints on the lowermost part of the measured section (Fig. 4), consideration of accumulation rates in comparable sectors of the fold-thrust belt ($50\text{--}100\text{ m Myr}^{-1}$; Horton, 2005) suggests that sedimentation likely began no earlier than $\sim 11\text{ Ma}$.

Sample 6070701 ($7.41 \pm 0.52\text{ Ma}$) demonstrates that basin filling continued for at least 1.5–3 Myr. An average sedimentation rate could not be determined due to a lack of precise stratigraphic correlations between the dated volcanic horizons. However, the new age constraints suggest

that Tipuani–Mapiri accumulation was synchronous with the late Miocene phase of exhumation in the Eastern Cordillera beginning at $\sim 11\text{ Ma}$ (Gillis *et al.*, 2006).

Finally, an early Miocene $^{40}\text{Ar}/^{39}\text{Ar}$ age for tuff sample M2006 ($22.11 \pm 0.18\text{ Ma}$) provides constraints on sedimentation in the Subandean Zone. The sample was collected from a clastic succession in the footwall of the CFP (Fig. 7). Although these deposits could be regarded as possible distal equivalents to the Tipuani–Mapiri basin, the sample is $> 10\text{ Myr}$ older. This discrepancy indicates a longer-lived Cenozoic accumulation history for this part of the Subandean Zone (Strub *et al.*, 2005), in contrast to the punctuated Tipuani–Mapiri accumulation along the Eastern Cordillera–Interandean Zone boundary.

DISCUSSION

Basin evolution and timing of shortening

Stratigraphic and sedimentologic observations combined with $^{40}\text{Ar}/^{39}\text{Ar}$ ages define the depositional systems and timing of sedimentation in the Tipuani–Mapiri basin (Fig. 2), placing limits on the shortening history of the central Andean fold-thrust belt. New $^{40}\text{Ar}/^{39}\text{Ar}$ results indicate sedimentation from at least 9.2 Ma until at least $\sim 7.4\text{ Ma}$, coeval with rapid late Miocene exhumation in the Eastern Cordillera that began at $\sim 11\text{ Ma}$ (Gillis *et al.*, 2006). Sedimentologic analyses reveal deposition principally by high-energy braided fluvial systems blanketing a palaeotopography with significant ($\sim 500\text{ m}$) relief (Fig. 9). Palaeocurrents and compositional data link coarse-grained sedimentation in the Tipuani–Mapiri basin to erosion of the deepest stratigraphic levels in the structural core of the Eastern Cordillera.

$^{40}\text{Ar}/^{39}\text{Ar}$ ages also provide timing constraints on upper-crustal shortening in the boundary zone between the Eastern Cordillera and Interandean Zone. Nearly flat-lying basin fill unconformably overlies a highly deformed Palaeozoic section and is not affected by mapped thrust faults cutting Palaeozoic rocks (Fig. 2). This contrast implies a change in deformation patterns upon initial accumulation in the Tipuani–Mapiri basin. These structural relationships and new $^{40}\text{Ar}/^{39}\text{Ar}$ results indicate that upper-crustal shortening along the Eastern Cordillera–Interandean Zone boundary was mostly complete by 11–9 Ma and the locus of deformation had advanced into the Subandean Zone.

Recent structural and thermochronologic analyses suggest that rapid late Miocene exhumation of the Eastern Cordillera occurred independently of upper-crustal shortening (Gillis *et al.*, 2006). We speculate that the Eastern Cordillera had achieved significant relief by late Miocene time and a climatic or deep crustal/lithospheric trigger potentially accounted for rapid erosion and an abrupt influx of coarse-grained sediment to the easternmost Eastern Cordillera, Interandean Zone and Subandean Zone.

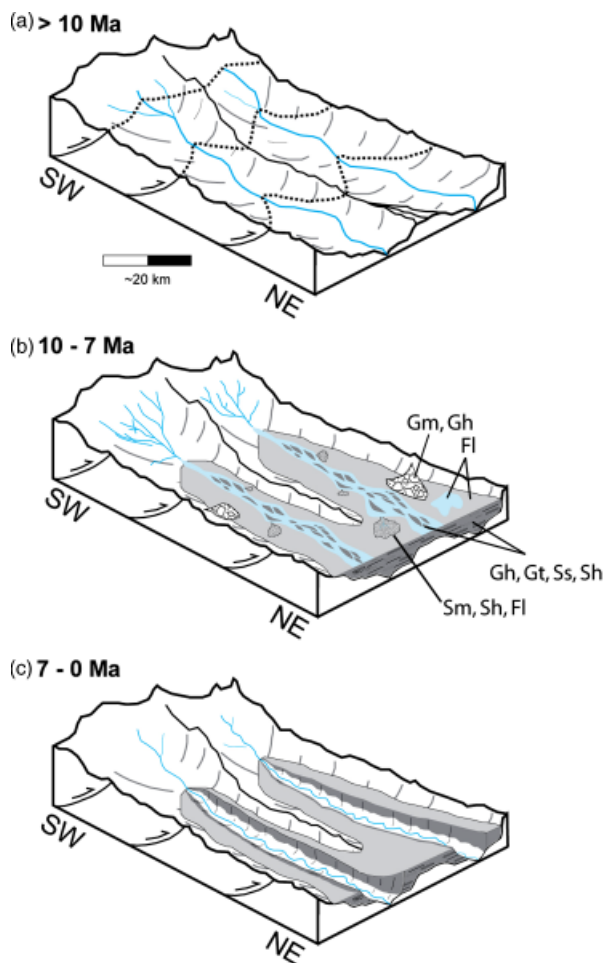


Fig. 9. Schematic geomorphic evolution of the Tipuani–Mapiri basin. (a) Thrusting and incision of Palaeozoic rocks along the Eastern Cordillera–Interandean Zone boundary before $\sim 10\text{ Ma}$. (b) Postshortening accumulation of sediment in the Tipuani–Mapiri basin at $\sim 10\text{--}7\text{ Ma}$, preserving an incised palaeotopography. (c) Postdepositional incision of the Tipuani–Mapiri basin at $\sim 7\text{--}0\text{ Ma}$.

Linkages among tectonics, climate and late Miocene sedimentation

Mechanisms of youthful exhumation in the Eastern Cordillera are not clear. Upper-crustal shortening ceased along much of the axis of the Bolivian Eastern Cordillera, including the Cordillera Real at 15.5–17.5°S, by early Miocene time (McQuarrie & DeCelles, 2001; Horton, 2005; Gillis *et al.*, 2006; McQuarrie *et al.*, 2008a). Relationships in the Tipuani-Mapiri basin show that shortening along the Eastern Cordillera–Interandean Zone boundary at 15–16°S was complete by 11–9 Ma. If upper-crustal shortening did not induce focused late Miocene exhumation of the Eastern Cordillera and corresponding rapid sedimentation in downslope regions, then alternative mechanisms

such as lower crustal/mantle processes and/or climate change seem to be required.

Possible deeper-level processes include basement duplexing (Sheffels, 1990; McQuarrie & DeCelles, 2001; McQuarrie, 2002; McQuarrie *et al.*, 2008a), steep basement faulting (Kley, 1996; Muller *et al.*, 2002), ductile thickening (Isacks, 1988; Gubbels *et al.*, 1993), tectonic underplating (Baby *et al.*, 1997) or removal of dense lithospheric mantle through delamination or other processes (Lamb & Hoke, 1997; Beck & Zandt, 2002; Garziona *et al.*, 2006, 2008). Regionally, the deep structure beneath the Eastern Cordillera shows evidence for piecemeal lithospheric removal (Myers *et al.*, 1998; Beck & Zandt, 2002), but the details beneath the Cordillera Real are poorly understood (Dorbath *et al.*, 1993, 1996).

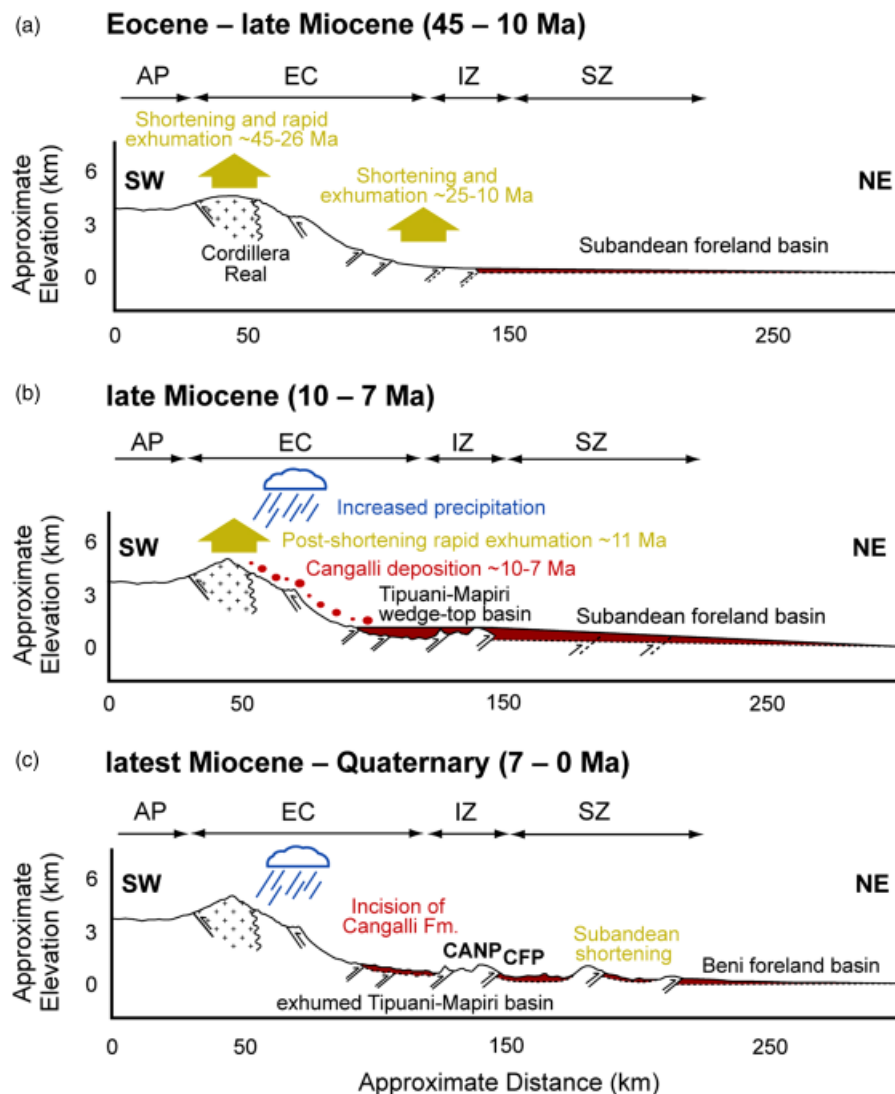


Fig. 10. Schematic cross sections depicting the timing of deformation, erosion and sedimentation in the central Andean fold-thrust belt at 15–16°S. Panels are based on topographic profile (Fig. 1) and principal structural elements (Fig. 2) of the Altiplano (AP), Eastern Cordillera (EC), Interandean Zone (IZ) and Subandean Zone (SZ). (a) Eocene–late Miocene: shortening and exhumation of the Eastern Cordillera and Interandean Zone, with foreland sedimentation in the Subandean region. (b) Late Miocene: increased precipitation and rapid exhumation in the Eastern Cordillera, with accumulation in the Tipuani-Mapiri basin coeval with a shift in upper-crustal shortening to the Subandean Zone. (c) Continued upper-crustal shortening in the Subandean Zone (CANP, Main Andean thrust; CFP, Main Frontal thrust) with postdepositional incision of the Tipuani-Mapiri basin.

Climate effects may also have been sufficient to drive late Miocene exhumation of the Eastern Cordillera independently of local crustal shortening. Climate modeling suggests that Andean climate changed significantly in response to orogenic plateau growth (Ehlers & Poulsen, 2009), potentially explaining isotopic shifts in the hinterland and foreland (Garziona *et al.*, 2006, 2008; Mulch *et al.*, 2010). In our simplified reconstruction (Fig. 10), large-magnitude shortening commencing in the Eocene (e.g. Horton, 2005; Gillis *et al.*, 2006; McQuarrie *et al.*, 2008a) led to crustal thickening and possible elevated topography. Surface uplift of the central Andes, whether triggered by gradual crustal thickening or abrupt lithospheric removal, influenced regional climate patterns, focusing precipitation along the orographic front of the Eastern Cordillera (e.g. Uba *et al.*, 2007). In turn, enhanced erosion and expansion of drainage networks during the late Miocene (e.g. Barnes & Heins, 2009; Mulch *et al.*, 2010) led to rapid exhumation of the Eastern Cordillera and evacuation of a huge volume of sediments deposited across the frontal part of the fold-thrust wedge and Andean foreland (Fig. 10).

Focused precipitation and erosion of the Eastern Cordillera (Masek *et al.*, 1994; Horton, 1999; Barnes & Pelletier, 2006) may have amplified sediment accumulation in the Interandean and Subandean zones. In the south, upper Miocene strata record a fourfold increase in sediment accumulation in the Andean foreland at $\sim 21^\circ\text{S}$, a pattern decoupled from shortening rates and attributed to regional climate variability and monsoon intensification (Uba *et al.*, 2007, 2009). In the north, Tipuani-Mapiri basin fill recorded an abrupt shift from erosional conditions to rapid late Miocene sedimentation within the frontal fold-thrust wedge. Rapid exhumation of the Eastern Cordillera starting at ~ 11 Ma (Gillis *et al.*, 2006) and contemporaneous high-energy fluvial systems in the Tipuani-Mapiri basin are consistent with an elevated source area exhibiting substantial palaeorelief by 11–9 Ma (Fig. 10).

Controls on basin accumulation

Basin filling could represent isolated intermontane basin development in the fold-thrust belt or integrated wedge-top deposition across a proximal foreland basin. In the former case, the Tipuani-Mapiri basin may match other intermontane basins in Bolivia which show structurally controlled axial fluvial drainages and ponded lacustrine systems (e.g. Horton, 1998, 2005; Sobel *et al.*, 2003). Alternatively, a wedge-top depozone (DeCelles & Giles, 1996; Horton & DeCelles, 1997) during the late Miocene may have covered part of the easternmost Eastern Cordillera, Interandean Zone and Subandean Zone, with a more distal region of foreland basin accumulation in the modern Beni (Amazon) plain (Fig. 1). Our results show sediment dispersal dominantly oriented to the NE (Fig. 5), transverse to major structural elements such as the CANP anticlinal ridge along the NE basin margin (Fig. 2). Although a min-

or structural influence may account for local axial (NW–SE) palaeocurrents, the dominance of transverse (NE-directed), high-energy braided fluvial systems with no indications of significant lacustrine sedimentation suggests continuous external drainage for the Tipuani-Mapiri basin. These lines of evidence, and the lack of observed growth strata, suggest a limited structural control for the late Miocene shift from an erosional to depositional regime along the Eastern Cordillera–Interandean Zone boundary. Moreover, the long-term record of Oligocene to Quaternary deposition in the Subandean Zone contrasts sharply with the Eastern Cordillera–Interandean Zone boundary, suggesting that punctuated late Miocene accumulation in the Tipuani-Mapiri basin may be driven by external factors, such as enhanced sediment delivery.

A model of an integrated wedge-top depozone (Fig. 10) is not only in better agreement with the palaeocurrent and facies information but also matches chronostratigraphic constraints on laterally equivalent strata of the Subandean Zone. Specifically, Strub *et al.* (2005) show that coarse-grained deposits in the proximal and distal parts of the Subandean Zone represent the downstream equivalents of the Cangalli Formation. Furthermore, a new $^{40}\text{Ar}/^{39}\text{Ar}$ biotite age of 8.7 ± 0.9 Ma for a tuff horizon in these Subandean deposits (Strub *et al.*, 2005) agrees remarkably well with the $^{40}\text{Ar}/^{39}\text{Ar}$ ages reported here for the Cangalli Formation. We suggest that focused late Miocene exhumation in the western Eastern Cordillera (Cordillera Real) led to a substantial influx of sediment that buried irregular topography in previously shortened regions along the Eastern Cordillera–Interandean Zone boundary and covered large tracts of the Subandean Zone. In our preferred reconstruction (Fig. 10), the resulting broad zone of wedge-top accumulation spanning the Tipuani-Mapiri region was contiguous with the central Andean foreland basin occupying the Subandean Zone and Beni plain. The fact that the termination of local shortening along the Eastern Cordillera–Interandean Zone coincided with the influx of wedge-top sediment and onset of accumulation in the Tipuani-Mapiri basin invites speculation that rapid sedimentation (and attendant loading) atop the Andean fold-thrust wedge promoted late Miocene advance of the thrust front in the Subandean Zone (e.g. Leturmy *et al.*, 2000; Uba *et al.*, 2009).

CONCLUSIONS

Sedimentology, stratigraphy, provenance and $^{40}\text{Ar}/^{39}\text{Ar}$ geochronology help link deposition in the Tipuani-Mapiri basin along the Eastern Cordillera–Interandean Zone boundary to focused late Miocene exhumation of the central Andean fold-thrust belt. Structural relationships demonstrate that considerable late Cenozoic exhumation of the lowest structural levels of the Eastern Cordillera occurred in the absence of local upper-crustal shortening, underscoring the need for alternative mechanisms such as climate change and/or deep crustal or lithospheric processes. The main conclusions are as follows.

- (1) Lithofacies associations identified in the Cangalli Formation indicate deposition primarily by high-energy braided fluvial systems, possibly in proximal zones of fluvial megafans. Stratigraphic and topographic relationships along the basal unconformity show that accumulation in the Tipuani–Mapiri basin occurred on an irregular, high-relief (~500 m) erosional surface developed on deformed Ordovician strata.
- (2) Palaeocurrents and compositional provenance data link deposition of the Cangalli Formation to erosion of the western Eastern Cordillera (Cordillera Real), the region of greatest structural relief within the central Andean fold–thrust belt. Late Miocene sedimentation in the Tipuani–Mapiri basin was coeval with rapid exhumation of this structural core of the orogen.
- (3) The Tipuani–Mapiri basin is dominated by subhorizontal strata (< 10° dip) with minimal evidence of deformation or tilting. The Cangalli Formation unconformably overlies a highly folded and faulted substrate of Ordovician rocks, indicating that shortening had ceased along the Eastern Cordillera–Interandean Zone boundary and migrated into the Subandean Zone by the late Miocene onset of basin filling.
- (4) ⁴⁰Ar/³⁹Ar age analyses of interbedded tuffs indicate that deposition in the Tipuani–Mapiri basin was underway by 11–9 Ma and continued until at least ~7.4 Ma. Evidence for transverse fluvial systems with limited influence by fold–thrust structures suggest that late Miocene accumulation occurred in a broad integrated wedge–top depozone of the proximal foreland basin spanning the easternmost Eastern Cordillera, Interandean Zone and Subandean Zone.
- (5) We propose that rapid erosional exhumation in the Eastern Cordillera was controlled by focused precipitation along the orographic front of the central Andean fold–thrust belt. Whether driven by climate change or by rapid surface uplift (possibly triggered by removal of lower crust or mantle lithosphere), higher precipitation likely increased sediment flux towards the foreland. This pulse of sediment may have promoted large-scale wedge–top deposition, enhancing sediment loading along the Eastern Cordillera–Interandean Zone boundary and potentially promoting rapid late Miocene advance of the deformation front in the Subandean fold–thrust system.

ACKNOWLEDGEMENTS

This research was partially supported by U.S. National Science Foundation grants EAR-0510441 and EAR-0908518 awarded to B. K. Horton, and graduate student research grants from the Geological Society of America and American Association of Petroleum Geologists awarded to J.G. Mosolf. We thank Sohrab Tawackoli, Raymond Ingersoll, Bryan Murray, Elizabeth Safran and Robert Gillis for beneficial discussions and Luke Wilson and Jaime Tito for field assistance. Constructive reviews by Jason Barnes,

Carmala Garizone, Thierry Sempere and editor Peter van der Beek improved the manuscript.

REFERENCES

- ALLMENDINGER, R.W., JORDAN, T.E., KAY, S.M. & ISACKS, B.L. (1997) The evolution of the Altiplano–Puna plateau of the central Andes. *Ann. Rev. Earth Planet. Sci.*, **25**, 139–174.
- BABY, P., ROCHAT, P., MASCLE, G. & HERAIL, G. (1997) Neogene shortening contribution to crustal thickening in the back arc of the Central Andes. *Geology*, **25**, 883–886.
- BARKE, R. & LAMB, S. (2006) Late Cenozoic uplift of the Eastern Cordillera, Bolivian Andes. *Earth Planet. Sci. Lett.*, **249**, 350–367.
- BARNES, J.B., EHLERS, T.A., MCQUARRIE, N., O’SULLIVAN, P.B. & PELLETIER, J.D. (2006) Eocene to recent variations in erosion across the central Andean fold–thrust belt, northern Bolivia: implications for plateau evolution. *Earth Planet. Sci. Lett.*, **248**, 118–133.
- BARNES, J.B., EHLERS, T.A., MCQUARRIE, N., O’SULLIVAN, P.B. & TAWACKOLI, S. (2008) Thermochronometer record of central Andean plateau growth, Bolivia (19.5 degrees S). *Tectonics*, **27**, TC3003, doi: 10.1029/2007TC002174.
- BARNES, J.B. & HEINS, J.D. (2009) Plio–Quaternary sediment budget between thrust belt erosion and foreland deposition in the central Andes, southern Bolivia. *Basin Res.*, **21**, 91–109.
- BARNES, J.B. & PELLETIER, J.D. (2006) Latitudinal variation of denudation in the evolution of the Bolivian Andes. *Am. J. Sci.*, **306**, 1–31.
- BECK, S.L. & ZANDT, G. (2002) The nature of orogenic crust in the central Andes. *J. Geophys. Res.–Solid Earth*, **107**(B10), 2230, doi: 10.1029/2000JB000124.
- BENJAMIN, M.T., JOHNSON, N.M. & NAESER, C.W. (1987) Recent rapid uplift in the Bolivian Andes: evidence from fission-track dating. *Geology*, **15**, 680–683.
- BLAIR, T.C. & MCPHERSON, J.G. (1992) The Trollheim alluvial–fan and facies model revisited. *Geol. Soc. Am. Bull.*, **104**, 762–769.
- BLAIR, T.C. & MCPHERSON, J.G. (1994) Alluvial fans and their natural distinction from rivers based on morphology, hydraulic processes, sedimentary processes, and facies assemblages. *J. Sediment. Res. Sec. A–Sediment. Petrol. Proc.*, **64**, 450–489.
- DECELLES, P.G. & GILES, K.A. (1996) Foreland basin systems. *Basin Res.*, **8**, 105–123.
- DECELLES, P.G. & HORTON, B.K. (2003) Early to middle Tertiary foreland basin development and the history of Andean crustal shortening in Bolivia. *Geol. Soc. Am. Bull.*, **115**, 58–77.
- DORBATH, C., GRANET, M., POUPINET, G. & MARTINEZ, C. (1993) A teleseismic study of the Altiplano and the Eastern Cordillera in northern Bolivia: new constraints on a lithospheric model. *J. Geophys. Res.–Solid Earth*, **98**, 9825–9844.
- DORBATH, C., PAUL, A., ACHAUER, U., ALDUNATE, M., BIANCHI, T., CAMINADE, J.P., FARRA, V., FONTANILLA, R., FORNARI, M., GUIGET, R., GUILBERT, J., GUILLIER, J., HERQUEL, G., LAMBERT, M., MARTINEZ, C., MASSON, F., MONFRET, T., PEQUEGNAT, C., SOLER, P. & WITTLINGER, G. (1996) Tomography of the Andean crust and mantle at 20 degrees S: first results of the lithoscope experiment. *Phys. Earth Planet. Interiors*, **97**, 133–144.
- EGE, H., SOBEL, E.R., SCHEUBER, E. & JACOBSHAGEN, V. (2007) Exhumation history of the southern Altiplano plateau (southern Bolivia) constrained by apatite fission track thermochronology. *Tectonics*, **26**, TC1004, doi: 10.1029/2005TC001869.

- EHLERS, T.A. & POULSEN, C.J. (2009) Influence of Andean uplift on climate and paleoaltimetry estimates. *Earth Planet. Sci. Lett.*, **281**, 238–248.
- ELGER, K., ONCKEN, O. & GLODNY, J. (2005) Plateau-style accumulation of deformation: southern Altiplano. *Tectonics*, **24**, TC4020, doi: 10.1029/2004TC001675.
- FARRAR, E., CLARK, A.H., KONTAK, D.J. & ARCHIBALD, D.A. (1988) Zongo–San Gaban Zone: eocene foreland boundary of the central Andean orogen, northwest Bolivia and southeast Peru. *Geology*, **16**, 55–58.
- FORNARI, M., HERAIL, G., VISCARA, G., LAUBACHER, G. & ARGOLLO, J. (1987) Sedimentation and structure of the Tipuani–Mapiro basin: a testimony to the Amazonian front evolution in the Andes of Bolivia. *C. R. Acad. Sci. Ser. II*, **305**, 1303–1308.
- GARZIONE, C.N., HOKE, G.D., LIBARKIN, J.C., WITHERS, S., MACFADDEN, B., EILER, J., GHOSH, P. & MULCH, A. (2008) Rise of the Andes. *Science*, **320**, 1304–1307.
- GARZIONE, C.N., MOLNAR, P., LIBARKIN, J.C. & MACFADDEN, B.J. (2006) Rapid late Miocene rise of the Bolivian Altiplano: evidence for removal of mantle lithosphere. *Earth Planet. Sci. Lett.*, **241**, 543–556.
- GILLIS, R.J., HORTON, B.K. & GROVE, M. (2006) Thermochronology, geochronology, and upper crustal structure of the Cordillera Real: implications for Cenozoic exhumation of the central Andean plateau. *Tectonics*, **25**, TC6007, doi: 10.1029/2005TC001887.
- GUBBELS, T.L., ISACKS, B.L. & FARRAR, E. (1993) High-level surfaces, plateau uplift, and foreland development, Bolivian Central Andes. *Geology*, **21**, 695–698.
- HERAIL, G., FORNARI, M., VISCARA, G., LAUBACHER, G., ARGOLLO, J. & MIRANDA, V. (1989) Geodynamic and gold distribution in the Tipuani–Mapiro basin (Bolivia). *International Symposium on Intermontane Basins: Geology & Resources*, Chiang Mai, Thailand.
- HERAIL, G., SHARP, W., GIOVANI, V. & FORNARI, M. (1994) La edad de la Formación Cangalli: Nuevos datos geocronológicos y su significado geológico. *Memorias del XI Congreso Geológico de Bolivia*, Santa Cruz, Bolivia.
- HORTON, B.K. (1998) Sediment accumulation on top of the Andean orogenic wedge: oligocene to late Miocene basins of the Eastern Cordillera, southern Bolivia. *Geol. Soc. Am. Bull.*, **110**, 1174–1195.
- HORTON, B.K. (1999) Erosional control on the geometry and kinematics of thrust belt development in the central Andes. *Tectonics*, **18**, 1292–1304.
- HORTON, B.K. (2005) Revised deformation history of the central Andes: inferences from Cenozoic foredeep and intermontane basins of the Eastern Cordillera, Bolivia. *Tectonics*, **24**, TC3011, doi: 10.1029/2003TC001619.
- HORTON, B.K. & DECELLES, P.G. (1997) The modern foreland basin system adjacent to the central Andes. *Geology*, **25**, 895–898.
- HORTON, B.K. & DECELLES, P.G. (2001) Modern and ancient fluvial megafans in the foreland basin system of the central Andes, southern Bolivia: implications for drainage network evolution in fold–thrust belts. *Basin Res.*, **13**, 43–63.
- HORTON, B.K., HAMPTON, B.A., LAREAU, B.N. & BALDELLON, E. (2002) Tertiary provenance history of the northern and central Altiplano (central Andes, Bolivia): a detrital record of plateau–margin tectonics. *J. Sediment. Res.*, **72**, 711–726.
- HORTON, B.K., HAMPTON, B.A. & WAANDERS, G.L. (2001) Paleogene synorogenic sedimentation in the Altiplano plateau and implications for initial mountain building in the central Andes. *Geol. Soc. Am. Bull.*, **113**, 1387–1400.
- ISACKS, B.L. (1988) Uplift of the central Andean plateau and bending of the Bolivian orocline. *J. Geophys. Res.–Solid Earth Planets*, **93**, 3211–3231.
- JONES, S.J., FROSTICK, L.E. & ASTIN, T.R. (2001) Braided stream and flood plain architecture: the Rio Vero Formation, Spanish Pyrenees. *Sediment. Geol.*, **139**, 229–260.
- KLEY, J. (1996) Transition from basement-involved to thin-skinned thrusting in the Cordillera Oriental of southern Bolivia. *Tectonics*, **15**, 763–775.
- KLEY, J. & MONALDI, C.R. (1998) Tectonic shortening and crustal thickness in the central Andes: how good is the correlation? *Geology*, **26**, 723–726.
- LAMB, S. & HOKE, L. (1997) Origin of the high plateau in the central Andes, Bolivia, South America. *Tectonics*, **16**, 623–649.
- LEIER, A.L., MCQUARRIE, N., HORTON, B.K. & GEHRELS, G.E. (2010) Upper Oligocene conglomerates of the Altiplano, central Andes: the record of deposition and deformation along the margin of a hinterland basin. *J. Sediment. Res.*, **80**, 750–762.
- LETURMY, P., MUGNIER, J.L., VINOUR, P., BABY, P., COLLETTA, B. & CHABRON, E. (2000) Piggyback basin development above a thin-skinned thrust belt with two detachment levels as a function of interactions between tectonic and superficial mass transfer: the case of the Subandean Zone (Bolivia). *Tectonophysics*, **320**, 45–67.
- LIMARINO, C., TRIPALDI, A., MARENSSI, S., NET, L., RE, G. & CASELLI, A. (2001) Tectonic control on the evolution of the fluvial systems of the Vinchina Formation (Miocene), northwestern Argentina. *J. S. Am. Earth Sci.*, **14**, 751–762.
- MACK, G.H., LEEDER, M., PEREZ-ARLUCEA, M. & BAILEY, B.D.J. (2003) Early Permian silt-bed fluvial sedimentation in the Orogande basin of the Ancestral Rocky Mountains, New Mexico, USA. *Sediment. Geol.*, **160**, 159–178.
- MARTINEZ, C. (1980) Structure et évolution de la chaîne hercynienne et de la chaîne andine dans le nord de la Cordillère des Andes de Bolivie. *Travaux et Documents de l'ORSTOM (Office de la Recherche Scientifique et Technique Outre-Mer)*, **119**, 352 pp.
- MASEK, J.G., ISACKS, B.L., GUBBELS, T.L. & FIELDING, E.J. (1994) Erosion and tectonics at the margins of continental plateaus. *J. Geophys. Res.–Solid Earth*, **99**, 13941–13956.
- MCBRIDE, S.L., ROBERTSON, R.C.R., CLARK, A.H. & FARRAR, E. (1983) Magmatic and metallogenic episodes in the northern tin belt, Cordillera–Real, Bolivia. *Geol. Rundsch.*, **72**, 685–713.
- MCQUARRIE, N. (2002) The kinematic history of the central Andean fold–thrust belt, Bolivia: implications for building a high plateau. *Geol. Soc. Am. Bull.*, **114**, 950–963.
- MCQUARRIE, N., BARNES, J.B. & EHLERS, T.A. (2008a) Geometric, kinematic, and erosional history of the central Andean plateau, Bolivia (15–17 degrees S). *Tectonics*, **27**, TC3007, doi: 10.1029/2006TC002054.
- MCQUARRIE, N. & DAVIS, G.H. (2002) Crossing the several scales of strain–accomplishing mechanisms in the hinterland of the central Andean fold–thrust belt, Bolivia. *J. Struct. Geol.*, **24**, 1587–1602.
- MCQUARRIE, N. & DECELLES, P. (2001) Geometry and structural evolution of the central Andean backthrust belt, Bolivia. *Tectonics*, **20**, 669–692.
- MCQUARRIE, N., EHLERS, T.A., BARNES, J.B. & MEADE, B. (2008b) Temporal variation in climate and tectonic coupling in the central Andes. *Geology*, **36**, 999–1002.
- MCQUARRIE, N., HORTON, B.K., ZANDT, G., BECK, S. & DECELLES, P.G. (2005) Lithospheric evolution of the Andean fold–thrust belt, Bolivia, and the origin of the central Andean plateau. *Tectonophysics*, **399**, 15–37.

- MIALL, A.D. (1977) Review of braided-river depositional environment. *Earth-Sci. Rev.*, **13**, 1–62.
- MIALL, A.D. (1985) Architectural-element analysis: a new method of facies analysis applied to fluvial deposits. *Earth-Sci. Rev.*, **22**, 261–308.
- MIALL, A.D. (1996) *The Geology of Fluvial Deposits*. Springer, New York.
- MONTGOMERY, D.R., BALCO, G. & WILLETT, S.D. (2001) Climate, tectonics, and the morphology of the Andes. *Geology*, **29**, 579–582.
- MULCH, A., UBA, C.E., STRECKER, M.R., SCHOENBERG, R. & CHAMBERLAIN, C.P. (2010) Late Miocene climate variability and surface elevation in the central Andes. *Earth Planet. Sci. Lett.*, **290**, 173–182.
- MULLER, J.P., KLEY, J. & JACOBSHAGEN, V. (2002) Structure and Cenozoic kinematics of the Eastern Cordillera, southern Bolivia (21 degrees S). *Tectonics*, **21**, 1037, doi: 10.1029/2001TC001340.
- MURRAY, B.P., HORTON, B.K., MATOS, R. & HEIZLER, M.T. (2010) Oligocene–Miocene basin evolution in the northern Altiplano, Bolivia: implications for evolution of the central Andean backthrust belt and high plateau. *Geol. Soc. Am. Bull.*, **122**, 1443–1462.
- MYERS, S.C., BECK, S., ZANDT, G. & WALLACE, T. (1998) Lithospheric-scale structure across the Bolivian Andes from tomographic images of velocity and attenuation for P and S waves. *J. Geophys. Res.-Solid Earth*, **103**, 21233–21252.
- NICHOLS, G.J. & FISHER, J.A. (2007) Processes, facies and architecture of fluvial distributary system deposits. *Sediment. Geol.*, **195**, 75–90.
- ROEDER, D. (1988) Andean-age structure of the Eastern Cordillera (Province of La-Paz, Bolivia). *Tectonics*, **7**, 23–39.
- SCHMITZ, M. (1994) A balanced model of the southern central Andes. *Tectonics*, **13**, 484–492.
- SEMPERE, T., HERAIL, G., OLLER, J. & BONHOMME, M.G. (1990) Late Oligocene–early Miocene major tectonic crisis and related basins in Bolivia. *Geology*, **18**, 946–949.
- SERVICIO GEOLOGICO DE BOLIVIA (GEOBOL). (1994) Carta Geologica de Bolivia, Chulumani (Hoja 6044), scale 1:100000, La Paz.
- SERVICIO GEOLOGICO DE BOLIVIA (GEOBOL). (1995) Carta Geologica de Bolivia, Milluni (Hoja 5945), scale 1:100000, La Paz.
- SERVICIO NACIONAL DE GEOLOGIA Y MINERIA. (1990) *Mapa geologico de Bolivia*. 1:1,000,000 scale, La Paz.
- SHEFFELS, B.M. (1990) Lower bound on the amount of crustal shortening in the central Bolivian Andes. *Geology*, **18**, 812–815.
- SOBEL, E.R., HILLEY, G.E. & STRECKER, M.R. (2003) Formation of internally drained contractional basins by aridity-limited bedrock incision. *J. Geophys. Res.-Solid Earth*, **108**(B7), 2344, doi: 10.1029/2002JB001883.
- STRUB, M., HERAIL, G., DARROZES, J., GARCIA-DUARTE, R. & ASTORGA, G. (2005) Neogene to present tectonic and orographic evolution of the Beni Subandean Zone. *6th International Symposium on Andean Geodynamics*, ISAG, Barcelona. Extended Abstracts, 709–713.
- UBA, C.E., HEUBECK, C. & HULKA, C. (2005) Facies analysis and basin architecture of the Neogene Subandean synorogenic wedge, southern Bolivia. *Sediment. Geol.*, **180**, 91–123.
- UBA, C.E., KLEY, J., STRECKER, M.R. & SCHMITT, A.K. (2009) Unsteady evolution of the Bolivian Subandean thrust belt: the role of enhanced erosion and clastic wedge progradation. *Earth Planet. Sci. Lett.*, **281**, 134–146.
- UBA, C.E., STRECKER, M.R. & SCHMITT, A.K. (2007) Increased sediment accumulation rates and climatic forcing in the central Andes during the late Miocene. *Geology*, **35**, 979–982.

Manuscript received 9 November 2009; In revised form 20 August 2010; Manuscript accepted 6 September 2010

SUPPORTING INFORMATION

Additional Supporting Information may be found in the online version of this article:

Table S1. $^{40}\text{Ar}/^{39}\text{Ar}$ analytical data.

Please note: Wiley-Blackwell is not responsible for the content or functionality of any supporting materials supplied by the authors. Any queries (other than missing material) should be directed to the corresponding author for the article.